Targeted Deletion of p53 Prevents Cardiac Rupture after Myocardial Infarction in Mice

Running title: p53 and myocardial infarction

Hidenori Matsusaka, Tomomi Ide, Shouji Matsushima, Masaki Ikeuchi, Toru Kubota, Kenji Sunagawa, Shintaro Kinugawa, Hiroyuki Tsutsui

Department of Cardiovascular Medicine (HM, TI, SM, MI, TK, KS), Graduate School of Medical Sciences, Kyushu University, Fukuoka 812-8582 and Department of Cardiovascular Medicine, Hokkaido University Graduate School of Medicine, Sapporo 060-8638 (SK, HT), Japan

Address for correspondence:

Hiroyuki Tsutsui, M.D., Ph.D.
Department of Cardiovascular Medicine,
Hokkaido University Graduate School of Medicine,
Kita-15, Nishi-7, Kita-ku, Sapporo 060-8638, Japan
Phone: +81-11-706-6970, FAX: +81-11-706-7874
e-mail: htsutsui@med.hokudai.ac.jp

Word count: 4850

1. Introduction

Myocardial infarction (MI) leads to complex structural alterations (remodeling) involving both the infarcted and noninfarcted left ventricular (LV) myocardium [1]. Early remodeling, which occurs during the early phase of MI, is characteristic for LV wall thinning and cavity dilatation in the infarct region (infarct expansion). Cardiac rupture is a lethal complication accounting for 5–30% of in-hospital mortality of MI [2] and is often associated with a transmural infarction, no prior history of angina pectoris, and a relatively large Q-wave infarct. Although the significance of these factors remains unestablished, accumulated lines of evidence have suggested that cardiac rupture results from the continuous stretch of infarcted and structurally weakened myocardium [3]. Recently, inflammatory cell infiltration and activation of matrix metalloproteinases (MMPs) have been also implicated in the pathogenesis of cardiac rupture [4, 5].

The tumor suppressor gene p53 is an important transcription factor regulating cell death and proliferation. It induces apoptosis in response to a variety of stresses such as ischemia [6, 7]. In fact, there is evidence supporting that p53 is activated in the ischemic hearts [8] and apoptotic myocytes are detected in the infarcted and border zone regions during the early days of MI [9, 10]. Based on these lines of evidence, we postulated that p53-dependent apoptosis might play an important role in early LV rupture after MI. However, no previous studies have yet determined the pathophysiological significance of p53 in this deleterious process. In the present study, we evaluated the effects of a targeted deletion of the p53 gene on the development of cardiac apoptosis and rupture after experimental MI in mice. To ensure selective and long-term complete inhibition of p53, we employed p53 knockout mice [11] because the most effective way to obtain the direct evidence for a role of p53 is through gene manipulation. We demonstrated that p53 was involved in cardiac rupture after

MI, probably via the induction of proapoptotic pathway. The inhibition of p53 may be a potentially useful therapeutic strategy to manage post-MI patients.

2. Methods

2.1. Animals

The study was approved by our Institutional Animal Research Committee and conformed with the *Guide for the Care and Use of Laboratory Animals* published by the US National Institutes of Health (NIH Publication No. 85-23, revised 1996). We used the progeny of homozygous p53 deficient mice ($p53^{-/-}$), heterozygous p53 deficient mice ($p53^{+/-}$), and their wild-type littermates ($p53^{+/+}$, C57BL/6J) ranging in age from 10 to 14 weeks old. $p53^{-/-}$ and $p53^{+/-}$ mice are viable, fertile, and indistinguishable from $p53^{+/+}$ mice in appearance but are prone to the spontaneous development of a variety of tumors by 6 months of age [12]. We thus assessed mice at the age of 10 to 14 weeks old for comparison between groups. The original breeding pairs used to develop the mice for this study were obtained from Jackson Laboratories (Bar Harbor, Maine). Genotypes of the mice were determined by PCR analyses of the mouse tail DNAs [13]. For p53, we used a sense oligonucleotide primer (5'-CCCGAGTATCTGGAAGACAG-3') and an antisense primer (5'-ATAGGTCGGCGGTTCAT-3'). For the neomycin cassette, we also used a sense oligonucleotide primer (5'-CTTGGGTGGAGAGGCTATTC-3') and an antisense primer (5'-AGGTGAGATGACAGGAGATC-3'). The amplicon from the WT allele is 600 bp, and the mutant allele is 280 bp (**Fig. 1**).

2.2. Creation of MI

We created MI in male $p53^{-/-}$ ($p53^{-/-}$+MI), $p53^{+/-}$ ($p53^{+/-}$+MI), and sibling wild-type mice ($p53^{+/+}$+MI) by ligating the left coronary artery [14]. A sham operation without coronary artery ligation was also performed in both $p53^{+/+}$ ($p53^{+/+}$+Sham) and $p53^{+/-}$ ($p53^{+/-}$+Sham) mice.

2.3. Experimental Protocol 1: 7 Day Post-MI Study

Survival

A survival analysis was performed for the $p53^{+/+}$+MI (n=29), $p53^{+/-}$+MI (n=28), and $p53^{-/-}$+MI (n=20) mice. During the 7-day study period, the cages were inspected daily to identify any deceased animals. All deceased mice were examined for the presence of MI as well as pleural effusion and cardiac rupture, based on a diagnosis of the presence of a blood clot within the chest cavity in the postmortem examination.

2.4. Experimental Protocol 2: 3 Day Post-MI Study

Because a substantial portion of the MI animals died within 7 days after MI, in vivo LV function and myocardial histopathology were also evaluated in a separate group of additional $p53^{-/-}$ ($p53^{-/-}$+MI), $p53^{+/-}$ ($p53^{+/-}$+MI), and sibling wild-type mice ($p53^{+/+}$+MI) at 3 days of surgery treated identically to experimental protocol 1. A sham operation without coronary artery ligation was also performed in both $p53^{+/+}$ ($p53^{+/+}$+Sham) and $p53^{+/-}$ ($p53^{+/-}$+Sham) mice. The numbers of $p53^{-/-}$ mice were less than those of $p53^{+/-}$ mice because of the limited number of $p53^{-/-}$ mice available for the detailed subsequent analysis. In fact, the previous study has shown that a significant proportion of female $p53^{-/-}$ mice die during embryogenesis or in the period between birth and weaning [15]. In addition, in $p53^{-/-}$ female embryos, the normal process of neural tube closure failed, leading to exencephaly and subsequent anencephaly. Another possible explanation for the lower availability of $p53^{-/-}$ mice is that p53 is involved in the normal process of spermatogenesis [16].

Echocardiographic and Hemodynamic Measurements

Echocardiographic studies were performed under light anesthesia with tribromoethanol/amylene hydrate (Avertin; 2.5% wt/vol, 8 μL/g ip) and spontaneous respiration [14]. A two-dimensional parasternal short-axis view of

the LV was obtained at the level of the papillary muscles. In general, the best views were obtained with the transducer lightly applied to the mid upper left anterior chest wall. The transducer was then gently moved cephalad or caudad and angulated until desirable images were obtained. After confirming that the imaging was on axis (based on roundness of the LV cavity), two-dimensional targeted M-mode tracings were recorded at a paper speed of 50 mm/sec. Next, a 1.4 Fr micromanometer-tipped catheter (Millar) was inserted into the right carotid artery and then was advanced into the left ventricle to measure the LV pressures. One subset of two investigators, who were not informed of the experimental groups, performed in vivo LV function studies. Our recent validation study has shown that the intraobserver and interobserver variabilities of our echocardiographic measurements for LV cavity dimensions and fractional shortening were small and measurements made in the same animals on separate days were highly reproducible [14].

Infarct Size and Wall Thickness

Infarct size was determined by the methods described in rats [17] and also in mice [18, 19]. The heart was excised and the right and left ventricles including the septum were dissected. The left ventricles were cut from apex to base into 3 transverse sections. Five-μm sections were cut and stained with Masson's trichrome. Infarct length was measured along the endo- and epicardial surfaces from each of the LV sections, and the values from all specimens were summed. Total LV circumference was calculated as the sum of endo- and epicardial segment lengths from all LV sections. Infarct size (in percent) was calculated as total infarct circumference dived by total LV circumference. In our preliminary study, we confirmed excellent reliability of infarct size measurements, in which a morphometric methodology similar to that used in this study was employed. The intraobserver and interobserver variabilities between two measurements divided by the mean of the two measurements,

expressed as a percentage, were less than 5%. Therefore, our technique could be considered to allow reliable assessment of infarct size in mice.

To further evaluate the effects of p53 on the risk area and infarct size, a separate group of animals including $p53^{+/-}$+MI (n=5) and $p53^{+/+}$+MI (n=5) was created. After 24 hr, Evans blue dye (1%) was perfused into the aorta and coronary arteries with distribution throughout the LV wall proximal to the site of coronary artery ligation. The nonischemic area was stained blue. Hearts were excised and sliced into cross-sections below the ligature. These sections were weighed and then incubated with a 1% triphenyltetrazolium chloride (TTC) solution at 37°C for 20 min. The infarct area (pale), the area at risk (not blue), and the total LV area from each section were measured, multiplied by the weight of the section, and then totaled from all sections [20].

To quantitate wall thinning, the thickness of the infarct wall was determined using the leading-edge method at the thinnest point of transmural infarction. The noninfarct wall measurement was then acquired from the same slide at the point on the LV diametrically opposed to the point used for infarct thinning. The wall thinning was calculated by dividing the infarct wall thickness by the noninfarct wall thickness [21, 22].

Myocardial Histopathology

From the mid-LV transverse sections, 5-μm sections were cut and stained with hematoxylin and eosin and Masson's trichrome. To quantify myocardial infiltrates, nuclear density (nuclei per square millimeter) was determined. In each animal, 5 independent high-powered fields were analyzed. To further determine the number of macrophages, an immunohistochemical analysis using a specific antibody against mouse Mac-3 (BD Pharmingen) was performed.

The collagen volume fraction was determined by the quantitative morphometry of Masson's trichrome-stained mid-LV sections. Interstitial

collagens were also stained with Sirius red.

MMP Zymography

Zymographic MMP levels including MMP-2 and MMP-9 were determined in the infarcted LV using gelatin zymography [23].

Apoptosis

To detect apoptosis, LV tissue sections were stained with terminal deoxynucleotidyl transferase-mediated dUTP nick end-labeling (TUNEL) staining (TaKaRa). The number of TUNEL-positive nuclei was counted in the infarcted and border zone LV, and the data were normalized per 10^5 total nuclei identified by hematoxylin-positive staining in the same sections. We further examined whether apoptosis is present by the more sensitive ligation-mediated PCR fragmentation assays (Maxim Biotech Inc.).

Akt Protein

The Akt protein levels were analyzed in cardiac tissue homogenates by Western blot analysis with a polyclonal antibody against phospho (Ser473)-Akt and Akt (Cell Signaling). In brief, the LV tissue was homogenized with the lysis buffer (25 mmol/L Tris, 150 mmol/L NaCl, 5 mmol/L EDTA, 1 mmol/L Na_3VO_4; pH 7.4). After centrifugation, equal amounts of protein (15 μg protein/lane), estimated by the Bradford method using a protein assay (Bio-Rad), were electrophoresed on a 12.5% SDS-polyacrylamide gel, and then electrophoretically transferred to a nitrocellulose membrane (Millipore). After blocking with 2.5% nonfat milk in TBS containing 0.1% Tween 20 at room temperature for 30 min, the membrane was incubated with the first antibody, and then with the peroxidase-linked second antibody (Santa Cruz). Chemiluminescence was detected with an ECL Western blot detection kit (Amersham Pharmacia) according to the manufacturer's recommendation.

2.5. Statistical Analysis

All data are expressed as the means±SEM. A survival analysis was performed by the Kaplan-Meier method, and between-group difference in survival was tested by the logrank test. Between-group comparisons of the means were performed by one-way ANOVA, followed by *t*-tests. The Bonferroni's correction was done for multiple comparisons of the means.

3. Results

3.1. Experimental Protocol 1: 7 Day Post-MI Study

Survival and LV Rupture

$p53^{+/-}$+MI and $p53^{-/-}$+MI mice had significantly better survival than $p53^{+/+}$+MI mice (**Fig. 2**). The number of the mice that died of LV rupture was significantly less in $p53^{-/-}$+MI and $p53^{+/-}$+MI than in $p53^{+/+}$+MI mice (**Fig. 3**). There were no deaths in the sham-operated groups. There were no significant differences in the survival rate among these 3 groups of survivor mice followed after 7 days up to 4 weeks.

3.2. Experimental Protocol 2: 3 Day Post-MI Study

Echocardiography and Hemodynamics

The echocardiographic and hemodynamic data of the surviving mice at 3 days of MI are shown in **Table 1**. The LV diameters increased and fractional shortening decreased significantly in the $p53^{+/+}$+MI, $p53^{+/-}$+MI, and $p53^{-/-}$+MI mice compared to sham operated mice. However, these changes were comparable among $p53^{+/+}$+MI, $p53^{+/-}$+MI, and $p53^{-/-}$+MI.

There was no significant difference in the heart rate and mean aortic blood pressure among 5 groups of mice. The LV end-diastolic pressure (EDP) increased and LV dP/dtmax decreased in $p53^{+/+}$+MI compared to sham, which was similarly observed in $p53^{+/-}$+MI and $p53^{-/-}$+MI.

Infarct Size and Wall Thickness

The infarct size determined by the morphometric analysis at 3 days of MI was comparable among the $p53^{+/+}$+MI, $p53^{+/-}$+MI, and $p53^{-/-}$+MI (n=6 each) mice **(Fig. 4A**). Moreover, percentages of LV at risk (risk area/LV; 60.4±5.2% vs 59.1±2.8%, *P*=NS) and the infarct size (infarct/risk area; 58.7±7.8% vs 61.4±2.5%, *P*=NS) measured by Evans blue and TTC staining at 24 hr of MI

were also comparable between $p53^{+/-}$+MI and $p53^{+/+}$+MI (n=5 each).

The thickness of the infarcted LV wall and that of the noninfarcted LV in $p53^{-/-}$+MI were 0.43±0.02 and 0.70±0.03 mm, respectively, those in $p53^{+/-}$+MI were 0.41±0.02 and 0.67±0.03 mm, respectively, and those in $p53^{+/+}$+MI were 0.39±0.01 and 0.70±0.02 mm, respectively. Thus infarct wall thinning ratio, the thickness of the infarcted LV wall normalized to that of the noninfarcted LV, was significantly greater in $p53^{-/-}$+MI or $p53^{+/-}$+MI than in $p53^{+/+}$+MI (**Fig. 4B**).

Myocardial Histopathology

MI mice had more infiltrating interstitial cells in the border zone and infarcted myocardium than sham-operated mice. However, the extent of infiltration was comparable among $p53^{+/+}$+MI, $p53^{+/-}$+MI, and $p53^{-/-}$+MI (**Fig. 5A**). Moreover, the infiltration of macrophages was similar between groups (**Fig. 5B**).

Interstitial fibrosis, measured as collagen volume fraction, in the infarcted as well as border zone LV was also comparable among $p53^{+/+}$+MI, $p53^{+/-}$+MI, and $p53^{-/-}$+MI (**Fig. 6A**).

MMPs

The zymographic MMP-2 and MMP-9 levels significantly increased in the infarcted LV from MI groups, however, no difference in this regard was seen between $p53^{+/+}$+MI and $p53^{+/-}$+MI mice (**Fig. 6B**).

Myocardial Apoptosis

There were rare TUNEL-positive nuclei in sham-operated mice. The number of TUNEL-positive cells was increased in $p53^{+/+}$+MI, which was significantly prevented in $p53^{+/-}$+MI and $p53^{-/-}$+MI (**Fig. 7A**). In addition, DNA ladder appeared faint in the infarcted LV from $p53^{+/-}$+MI compared to that from

$p53^{+/+}$+MI (**Fig. 7B**).

Akt Protein

Either Akt protein (total) or phospho-Akt levels did not differ between 4 groups of $p53^{+/+}$+Sham, $p53^{+/-}$+Sham, $p53^{+/+}$+MI, and $p53^{+/-}$+MI mice (**Fig. 8**).

4. Discussion

The major new finding of the present study is the significant improvement in the survival of MI mice by the targeted deletion of p53 gene, which was mainly attributable to the inhibition of early LV rupture. After MI, p53-dependent apoptosis might contribute to the thinning of the infarct wall and eventual LV rupture. Our observations thus suggest that an anti-p53 strategy may be of therapeutic benefit against the evolution of cardiac rupture after MI.

Cardiac rupture is the most drastic and severe complication of acute MI. Following MI, a reparative process, infarct healing, is immediately initiated, including inflammatory cell infiltration, activation of MMPs, extracellular matrix remodeling and scar formation. Thinning of the infarcted wall and dilatation of LV cavity, which occur during the acute phase of MI, are termed as "infarct expansion" [1]. The delay or impairment of this process may jeopardize infarct healing, aggravate extracellular matrix remodeling, and cause cardiac rupture. Previous studies demonstrated that p53 was increased [8] and apoptosis of cardiac myocytes were detected in the infarcted regions during the early days after MI [9, 10]. Therefore, p53-dependent apoptosis at the infarcted myocardium may contribute to cardiac rupture. However, no previous studies have provided direct evidence supporting this notion. The present study has demonstrated that p53 is indeed involved in cardiac rupture after MI (**Fig. 3**) via mediating apoptosis (**Fig. 7**) and wall thinning at the infarct area (**Fig. 4B**).

The beneficial effects of p53 deletion were not due to its MI size-sparing effects because the infarct size was comparable between the $p53^{+/+}$ and $p53^{+/-}$ mice (**Fig. 4A**). Further, its effects might not be attributable to those on hemodynamics because the blood pressure and heart rate showed no alterations (**Table 1**). In addition, inflammatory cell infiltration and inadequate fibrosis have been postulated to cause myocyte separation in the infarct area, which may lead to eventual cardiac rupture [4]. However, the present study could not find

any alterations in the infiltration of inflammatory cells or collagen deposition between $p53^{+/+}$ and $p53^{+/-}$ mice after MI (**Fig. 5 and 6A**). Further, even though recent studies have demonstrated that the inhibition of MMPs can prevent cardiac rupture [4, 5], targeted deletion of p53 gene did not affect the increase in MMP-2 or MMP-9 activities in the post-MI hearts in the present study (**Fig. 6B**). These lines of evidence indicate that the inhibition of cardiac rupture in $p53^{+/-}$ mice was not due to the altered reparative process of extracellular matrix or the infiltration of inflammatory cells and further confirm the significance of attenuated apoptosis and infarct wall thinning in the prevention of cardiac rupture.

Previous experimental [9] and human [10] studies have detected TUNEL-positive cells in the post-MI hearts. Even though they implicated apoptosis in the pathogenesis of late LV remodeling after MI [19], it may also contribute to the early phase structural alterations known to occur within the infarct area, which is characterized by a significant net loss of cardiac myocytes as well as myocyte slippage and elongation [24]. However, the significance of myocardial apoptosis in this phase of MI has been mostly speculative. Thus the present study clearly demonstrated for the first time that p53-dependent apoptosis is involved not only in late remodeling after MI [19] but also in early cardiac rupture.

The present study was in contrast to the previous study by Bialik et al, in which myocyte apoptosis was not altered after MI in the hearts of mice nullizygous for p53 [25]. It is difficult, however, to find identical experimental conditions between their study and the present study by that would be necessary for a direct comparison; the age of the animals (6-8 weeks in the study by Bialik vs 10-14 weeks in this study) and the time at which apoptosis was assessed (10 and 48 hr vs. 3 days). In addition, the infarct size was comparable between $p53^{-/-}$ and $p53^{+/-}$ in the present study although it was not clearly mentioned in the study by Bialik. Although the present study demonstrated the survival benefit in p53

deletion, no survival data were provided in their study.

p53 is known to be dynamically regulated via Akt, a serine/threonine kinase, that promotes cell survical [26]. Specifically, proapoptoitc stimulation leads to p53-dependent destruction of Akt whereas Akt activation leads to inhibition of p53. The state of this signaling network determines the fate of the cell to survive or to enter apoptosis or hypertrophy. However, either Akt protein (total) or phospho-Akt levels did not differ between 4 groups of $p53^{+/+}$+Sham, $p53^{+/-}$+Sham, $p53^{+/+}$+MI, and $p53^{+/-}$+MI mice in the present study (**Fig. 8**), suggesting that Akt might not play a major role in myocyte apoptosis in this model. Moreover, a recent study by Dr. Field's group has demonstrated that p193 and p53 exert a cell cycle regulatory role in the adult heart [27]. In their studies, target expression of the p193 and/or the p53 dominant-interfering mutants increased cardiac myocyte DNA synthesis after MI in mice, suggesting that cardiac cell cycle reentry is regulated by these proapoptoitc proteins. Therefore, we could not exclude the possibility that p193 might be also involved in post-MI remodeling.

Even though the previous studies reported a difference in the phenotype between $p53^{-/-}$ and $p53^{+/-}$ mice [15, 16], the echocardiographic data (**Table 1),** hemodynamic data (**Table 1**), infarct size (**Fig. 4**), infarct wall thinning ratio (**Fig. 4**), nuclear density (**Fig. 5**), collagen volume fraction by myocardial histopathology (**Fig. 6**), and the number of TUNEL-positive cells (**Fig. 7**) were comparable between these 2 groups of mice in the present study. Based on these results, there might be a threshold in the effects of p53 gene expression on cardiac pathophysiology after MI.

There are several limitations to be acknowledged in this study. First, although p53 is activated in the post-MI hearts [8], the mechanisms responsible for this activation are not determined in the present study. One important aspect of ischemia is prolonged hypoxia, which has been shown to increase p53 expression and result in apoptosis in cultured cardiac myocytes [6]. Furthermore,

oxidative stress, which is also increased in post-MI hearts, is a powerful inducer of apoptosis [28]. However, further studies are needed to clarify the mechanisms for the modulation of p53 after MI. Second, even though the previous study demonstrated that p53 expression was increased in post-MI rat hearts [8], the present study did not determine whether endogenous p53 expression was altered in post-MI mouse hearts. Third, p53-dependent apoptotic pathways may not be a sole mechanism for cardiac rupture after MI. Cardiac repair after MI is a highly complex process, involving diverse inflammatory and growth factor signaling pathways, and extracellular matrix remodeling. Thus the mechanisms other than p53 may be also involved in this deleterious complication. Fourth, echocardiographic assessment of LV function in mice is known to be difficult. However, intra- and interobserver variabilities of our echocardiographic measurements for LV cavity dimensions and fractional shortening were small and measurements were highly reproducible [14]. Therefore, our technique was capable of noninvasively assessing the LV structure and function in mice with a large MI.

Cardiac rupture usually occurs unexpectedly and is often fatal, thereby resulting in one of the major causes of in-hospital death in patients with acute MI. It is difficult to predict its occurrence by the previously reported clinical risk factors such as aging, hypertension, and delayed thrombolysis [29]. We found that target deletion of p53 had a significantly reduced cardiac rupture rate after MI. This was accompanied by a reduction of apoptosis and wall thinning of the infarcted myocardium. Our results may provide a novel insight regarding the pathophysiological role of p53-dependent apoptosis in cardiac rupture and thus help to establish an effective therapeutic strategy.

Acknowledgments

This study was supported in part by grants from the Ministry of Education, Science and Culture (No. 120670676, 14370230, 17390223). A part of this study was conducted in Kyushu University Station for Collaborative Research I and II.

References

[1] Pfeffer JM, Pfeffer MA, Fletcher PJ, Braunwald E. Progressive ventricular remodeling in rat with myocardial infarction. Am J Physiol 1991;260:H1406-14.

[2] Anzai T, Yoshikawa T, Shiraki H, Asakura Y, Akaishi M, Mitamura H, et al. C-reactive protein as a predictor of infarct expansion and cardiac rupture after a first Q-wave acute myocardial infarction. Circulation 1997;96:778-84.

[3] Przyklenk K, Connelly CM, McLaughlin RJ, Kloner RA, Apstein CS. Effect of myocyte necrosis on strength, strain, and stiffness of isolated myocardial strips. Am Heart J 1987;114:1349-59.

[4] Heymans S, Luttun A, Nuyens D, Theilmeier G, Creemers E, Moons L, et al. Inhibition of plasminogen activators or matrix metalloproteinases prevents cardiac rupture but impairs therapeutic angiogenesis and causes cardiac failure. Nat Med 1999;5:1135-42.

[5] Matsumura S, Iwanaga S, Mochizuki S, Okamoto H, Ogawa S, Okada Y. Targeted deletion or pharmacological inhibition of MMP-2 prevents cardiac rupture after myocardial infarction in mice. J Clin Invest 2005;115:599-609.

[6] Long X, Boluyt MO, Hipolito ML, Lundberg MS, Zheng JS, O'Neill L, et al. p53 and the hypoxia-induced apoptosis of cultured neonatal rat cardiac myocytes. J Clin Invest 1997;99:2635-43.

[7] Polyak K, Xia Y, Zweier JL, Kinzler KW, Vogelstein B. A model for p53-induced apoptosis. Nature 1997;389:300-5.

[8] Oskarsson HJ, Coppey L, Weiss RM, Li WG. Antioxidants attenuate myocyte apoptosis in the remote non-infarcted myocardium following large myocardial infarction. Cardiovasc Res 2000;45:679-87.

[9] Kajstura J, Cheng W, Reiss K, Clark WA, Sonnenblick EH, Krajewski S,

et al. Apoptotic and necrotic myocyte cell deaths are independent contributing variables of infarct size in rats. Lab Invest 1996;74:86-107.

[10] Saraste A, Pulkki K, Kallajoki M, Henriksen K, Parvinen M, Voipio-Pulkki LM. Apoptosis in human acute myocardial infarction. Circulation 1997;95:320-3.

[11] Mayr U, Mayr M, Li C, Wernig F, Dietrich H, Hu Y, et al. Loss of p53 accelerates neointimal lesions of vein bypass grafts in mice. Circ Res 2002;90:197-204.

[12] Donehower LA, Harvey M, Slagle BL, McArthur MJ, Montgomery CA, Jr., Butel JS, et al. Mice deficient for p53 are developmentally normal but susceptible to spontaneous tumours. Nature 1992;356:215-21.

[13] Ducharme A, Frantz S, Aikawa M, Rabkin E, Lindsey M, Rohde LE, et al. Targeted deletion of matrix metalloproteinase-9 attenuates left ventricular enlargement and collagen accumulation after experimental myocardial infarction. J Clin Invest 2000;106:55-62.

[14] Shiomi T, Tsutsui H, Hayashidani S, Suematsu N, Ikeuchi M, Wen J, et al. Pioglitazone, a peroxisome proliferator-activated receptor-gamma agonist, attenuates left ventricular remodeling and failure after experimental myocardial infarction. Circulation 2002;106:3126-32.

[15] Armstrong JF, Kaufman MH, Harrison DJ, Clarke AR. High-frequency developmental abnormalities in p53-deficient mice. Curr Biol 1995;5:931-6.

[16] Rotter V, Schwartz D, Almon E, Goldfinger N, Kapon A, Meshorer A, et al. Mice with reduced levels of p53 protein exhibit the testicular giant-cell degenerative syndrome. Proc Natl Acad Sci U S A 1993;90:9075-9.

[17] Pfeffer MA, Pfeffer JM, Fishbein MC, Fletcher PJ, Spadaro J, Kloner RA, et al. Myocardial infarct size and ventricular function in rats. Circ Res 1979;44:503-12.

[18] Patten RD, Aronovitz MJ, Deras-Mejia L, Pandian NG, Hanak GG, Smith

JJ, et al. Ventricular remodeling in a mouse model of myocardial infarction. Am J Physiol 1998;274:H1812-20.

[19] Sam F, Sawyer DB, Chang DL, Eberli FR, Ngoy S, Jain M, et al. Progressive left ventricular remodeling and apoptosis late after myocardial infarction in mouse heart. Am J Physiol Heart Circ Physiol 2000;279:H422-8.

[20] Ikeuchi M, Tsutsui H, Shiomi T, Matsusaka H, Matsushima S, Wen J, et al. Inhibition of TGF-beta signaling exacerbates early cardiac dysfunction but prevents late remodeling after infarction. Cardiovasc Res 2004;64:526-35.

[21] Delyani JA, Robinson EL, Rudolph AE. Effect of a selective aldosterone receptor antagonist in myocardial infarction. Am J Physiol Heart Circ Physiol 2001;281:H647-54.

[22] Lindsey ML, Gannon J, Aikawa M, Schoen FJ, Rabkin E, Lopresti-Morrow L, et al. Selective matrix metalloproteinase inhibition reduces left ventricular remodeling but does not inhibit angiogenesis after myocardial infarction. Circulation 2002;105:753-8.

[23] Hayashidani S, Tsutsui H, Ikeuchi M, Shiomi T, Matsusaka H, Kubota T, et al. Targeted deletion of MMP-2 attenuates early LV rupture and late remodeling after experimental myocardial infarction. Am J Physiol Heart Circ Physiol 2003;285:H1229-35.

[24] Li Q, Li B, Wang X, Leri A, Jana KP, Liu Y, et al. Overexpression of insulin-like growth factor-1 in mice protects from myocyte death after infarction, attenuating ventricular dilation, wall stress, and cardiac hypertrophy. J Clin Invest 1997;100:1991-9.

[25] Bialik S, Geenen DL, Sasson IE, Cheng R, Horner JW, Evans SM, et al. Myocyte apoptosis during acute myocardial infarction in the mouse localizes to hypoxic regions but occurs independently of p53. J Clin Invest 1997;100:1363-72.

[26] Sussman MA, Anversa P. Myocardial aging and senescence: where have the stem cells gone? Annu Rev Physiol 2004;66:29-48.

[27] Nakajima H, Nakajima HO, Tsai SC, Field LJ. Expression of mutant p193 and p53 permits cardiomyocyte cell cycle reentry after myocardial infarction in transgenic mice. Circ Res 2004;94:1606-14.

[28] von Harsdorf R, Li PF, Dietz R. Signaling pathways in reactive oxygen species-induced cardiomyocyte apoptosis. Circulation 1999;99:2934-41.

[29] Maggioni AP, Maseri A, Fresco C, Franzosi MG, Mauri F, Santoro E, et al. Age-related increase in mortality among patients with first myocardial infarctions treated with thrombolysis. The Investigators of the Gruppo Italiano per lo Studio della Sopravvivenza nell'Infarto Miocardico (GISSI-2). N Engl J Med 1993;329:1442-8.

Figure legends

Figure 1 PCR genotyping of $p53^{+/+}$, $p53^{+/-}$, and $p53^{-/-}$ mice. The amplicon from the WT allele is 600 bp, and the mutant allele is 280 bp. M, marker.

Figure 2 Kaplan-Meier analysis of survival after MI in $p53^{+/+}$+MI (n=29), and $p53^{+/-}$+MI (n=28), and $p53^{-/-}$+MI (n=20) mice. There was no death after the sham operation in $p53^{+/+}$ and $p53^{+/-}$ mice (data not shown). **P*<0.05 for difference from the $p53^{+/+}$+MI.

Figure 3 The number of animals died of cardiac rupture in the $p53^{+/+}$+MI, $p53^{+/-}$+MI, and $p53^{-/-}$+MI mice.

Figure 4 Infarct size (A) and infarct wall thinning ratio (B) in $p53^{+/+}$-MI, $p53^{+/-}$-MI, and $p53^{-/-}$-MI mice (n=6 each). Values are means±SEM. **P*<0.05 for difference from the $p53^{+/+}$+MI.

Figure 5 Representative photomicrographs of LV sections and summary data for nuclear density of infiltrating cells stained with hematoxylin and eosin (A) and macrophages (B) at the infarct area and border zone. Scale bar, 10 μm. Values are means±SEM (n=6 each).

Figure 6 **A,** Summary data of collagen volume fraction at the infarcted area and border zone of LV tissue sections (n=6 for each). **B,** Representative LV zymographic MMP-2 and MMP-9 levels and summary data at 3 days of MI (n=6 for each).

Figure 7 **A,** Representative photomicrographs of LV sections and

summary data for the number of TUNEL-positive cells in the infarcted area and border zone of LV (n=6 each). Scale bar, 10 μm. Values are means±SEM. **P*<0.05, ***P*<0.01 for difference from the $p53^{+/+}$+MI values. **B,** DNA ladder indicative of apoptosis in the genomic DNA from the LV. M, marker. P, positive control.

Figure 8 **A,** Representative Western blot analysis of Akt (total) and phospho-Akt protein levels in LV tissue obtained from 4 groups of $p53^{+/+}$+Sham, $p53^{+/-}$+Sham, $p53^{+/+}$+MI, and $p53^{+/-}$+MI mice. Summary data for total Akt (**B**) and phospho-Akt (**C**) protein levels in $p53^{+/+}$+Sham, $p53^{+/-}$+Sham, $p53^{+/+}$+MI, and $p53^{+/-}$+MI mice (n=3 for each). M, marker.

Fig.1

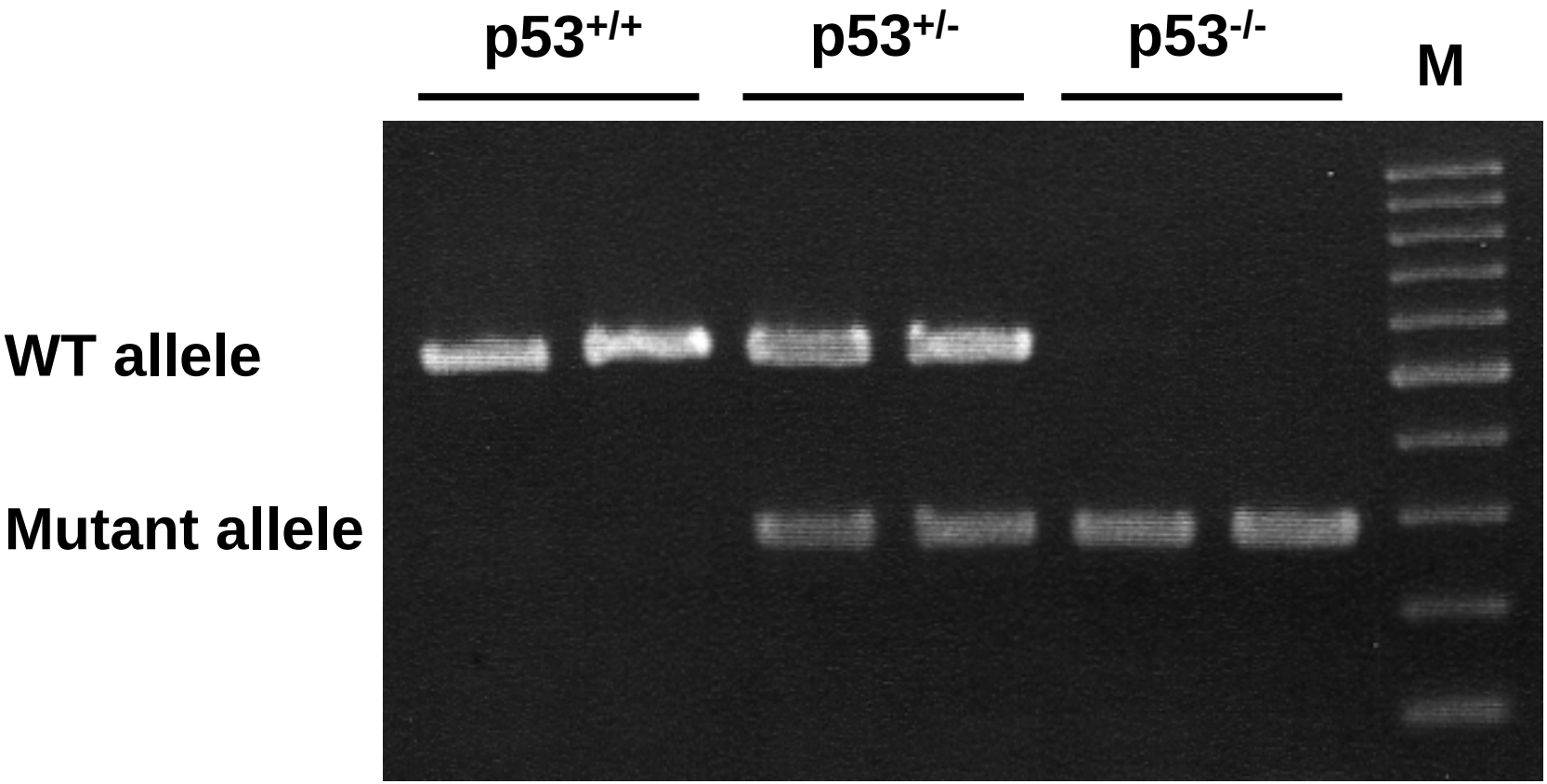

Fig.2

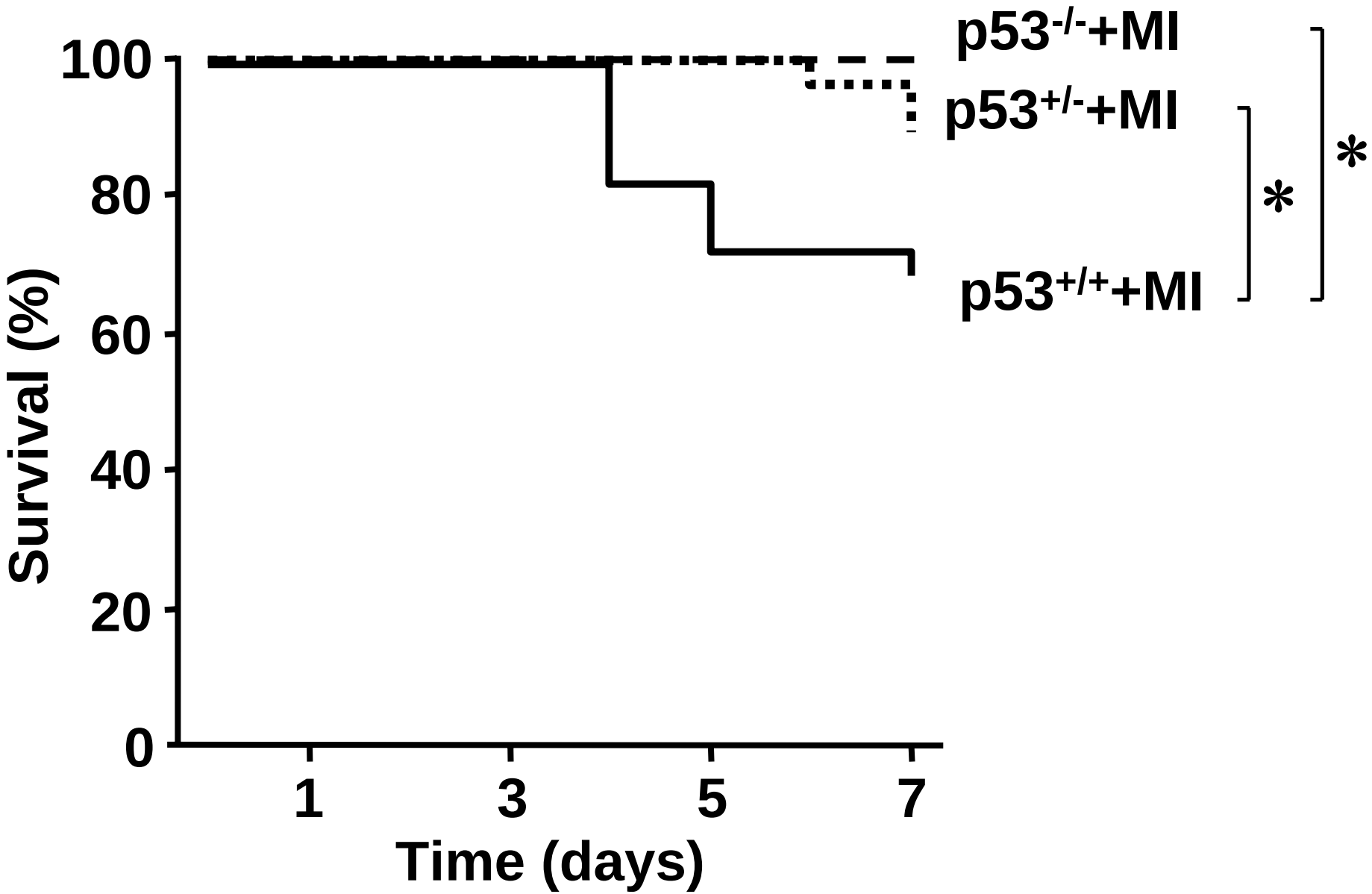

Fig.3

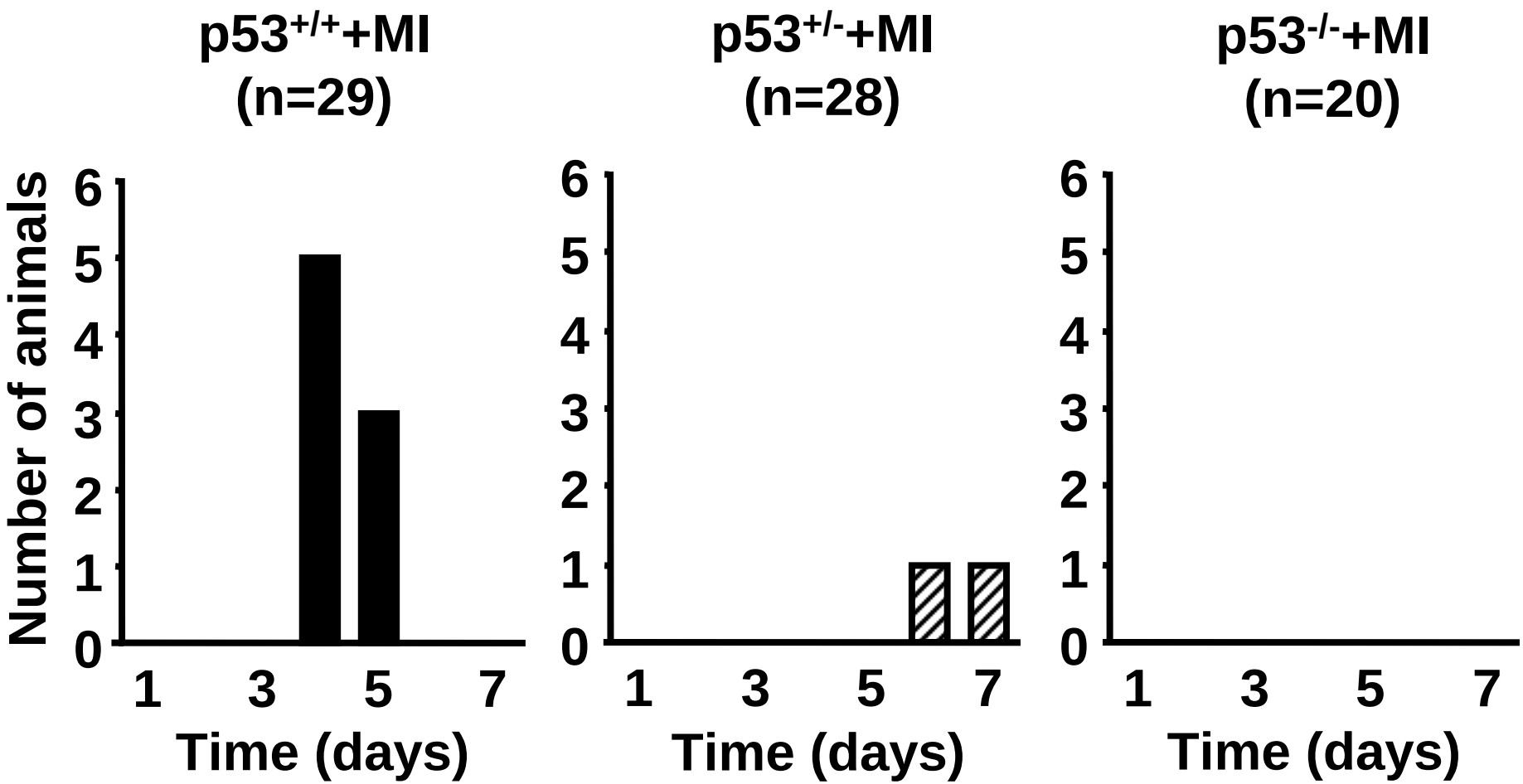
p53+/+ +MI
(n=29)
p53+/- +MI
(n=28)
p53-/- +MI
(n=20)
Number of animals
0
1
2
3
4
5
6
1
3
5
7
Time (days)

Fig.4

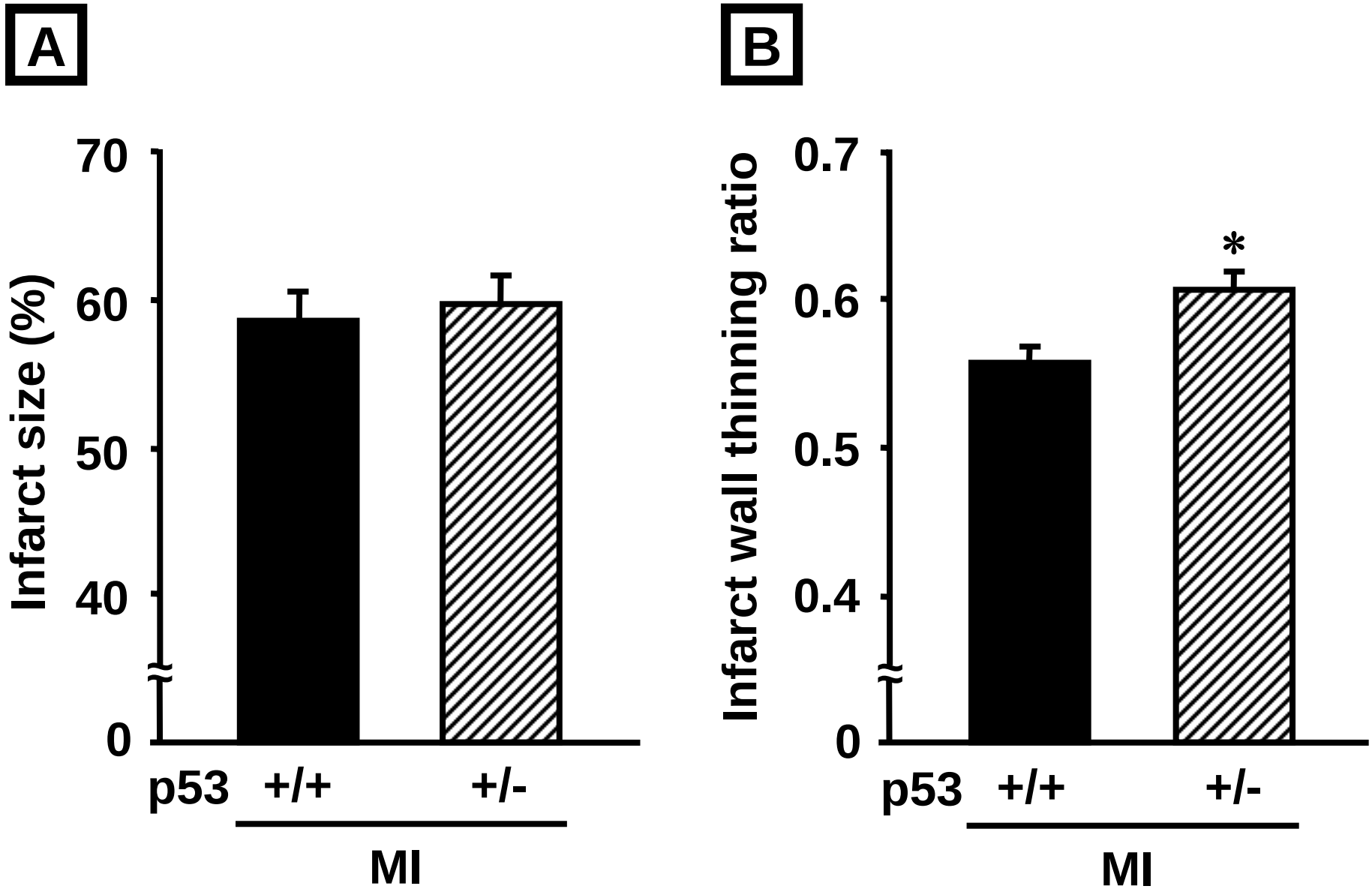
A
Infarct size (%)
70
60
50
40
0
p53
+/+
+/-
MI
B
Infarct wall thinning ratio
0.7
0.6
0.5
0.4
0
*
p53
+/+
+/-
MI

Fig.5

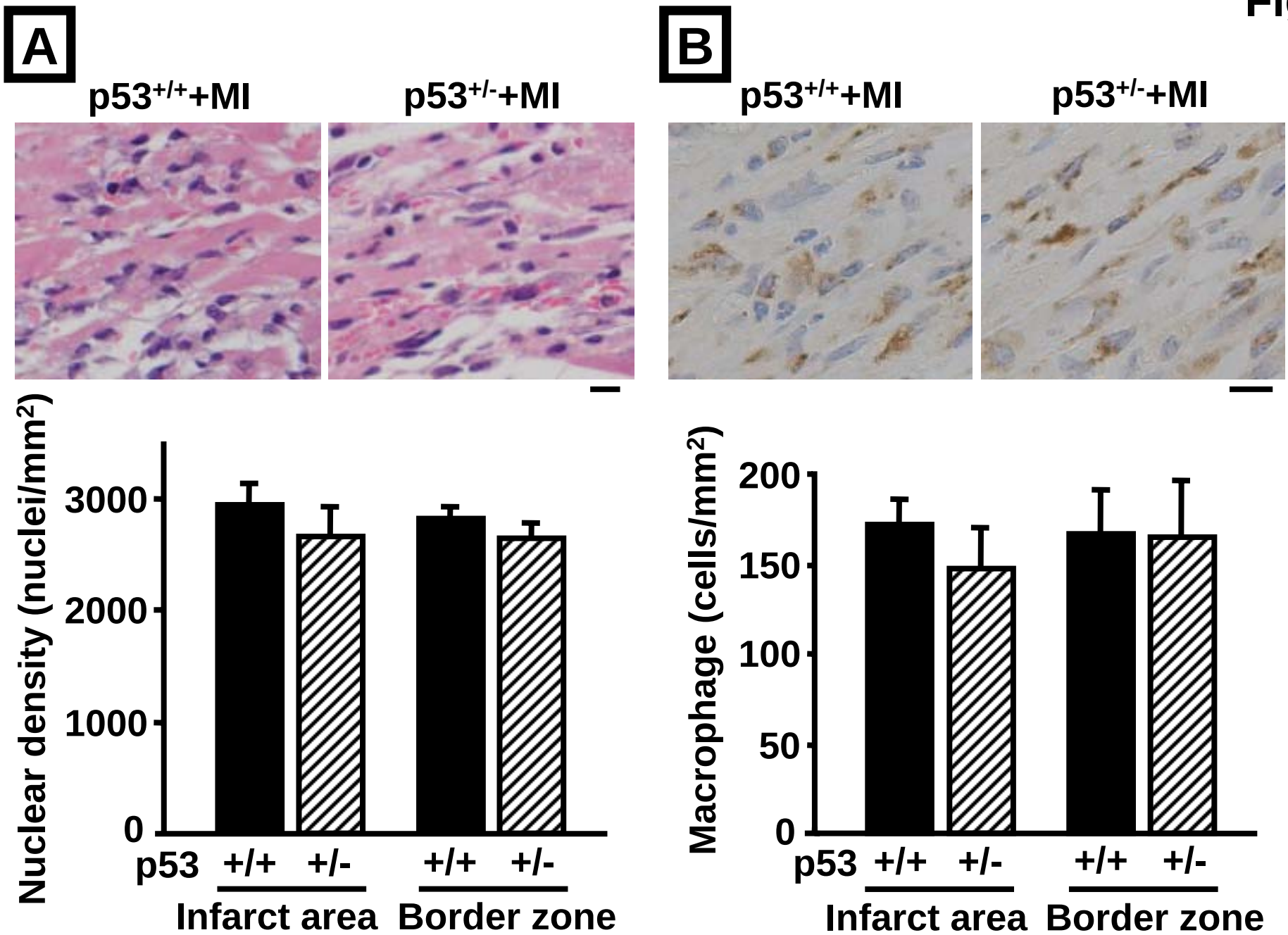
A
p53+/++MI
p53+/-+MI
B
p53+/++MI
p53+/-+MI
Nuclear density (nuclei/mm2)
3000
2000
1000
0
p53 +/+ +/- +/+ +/-
Infarct area
Border zone
Macrophage (cells/mm2)
200
150
100
50
0
p53 +/+ +/- +/+ +/-
Infarct area
Border zone

Fig.6

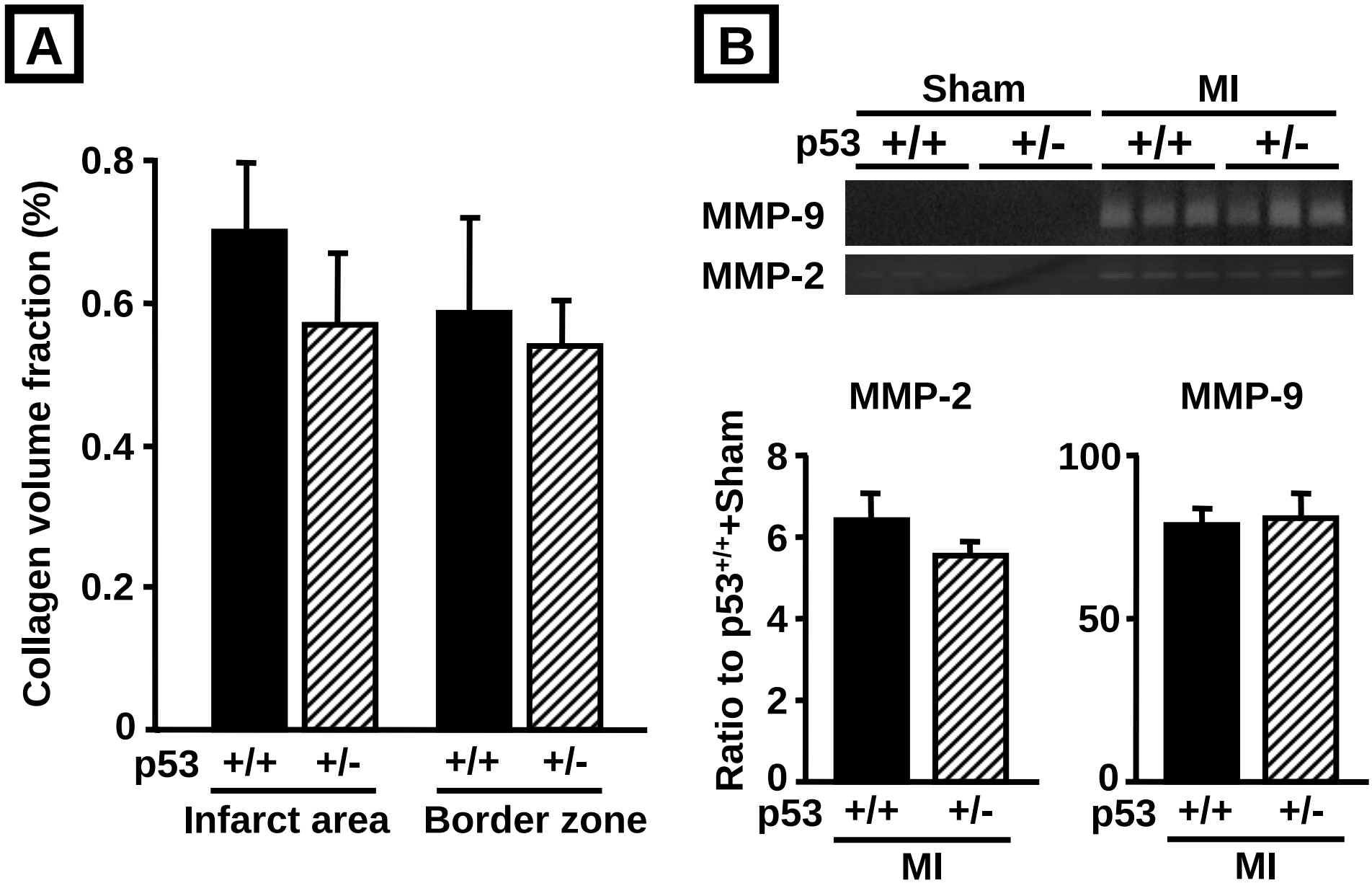
A
Collagen volume fraction (%)
0.8
0.6
0.4
0.2
0
p53 +/+ +/- +/+ +/-
Infarct area
Border zone
B
Sham
MI
p53 +/+ +/- +/+ +/-
MMP-9
MMP-2
MMP-2
MMP-9
Ratio to p53+/++Sham
8
6
4
2
0
100
50
0
p53 +/+ +/-
MI
p53 +/+ +/-
MI

Fig.7

A

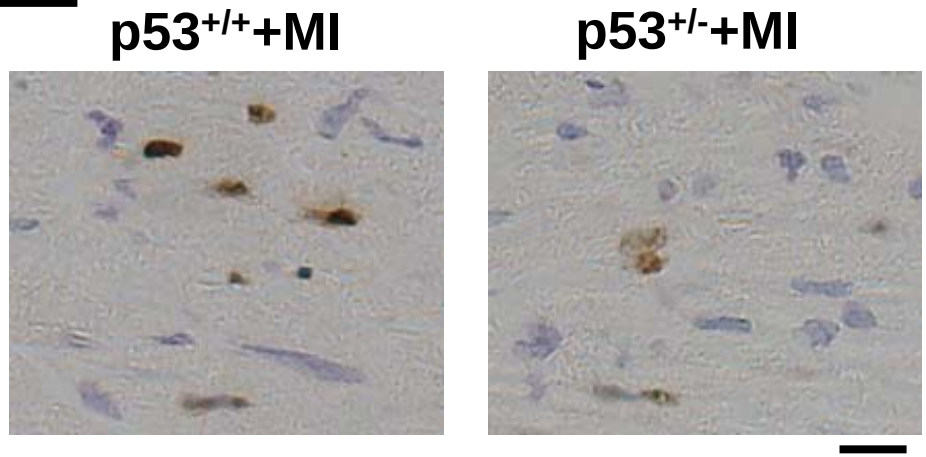
p53+/+ +MI
p53+/- +MI

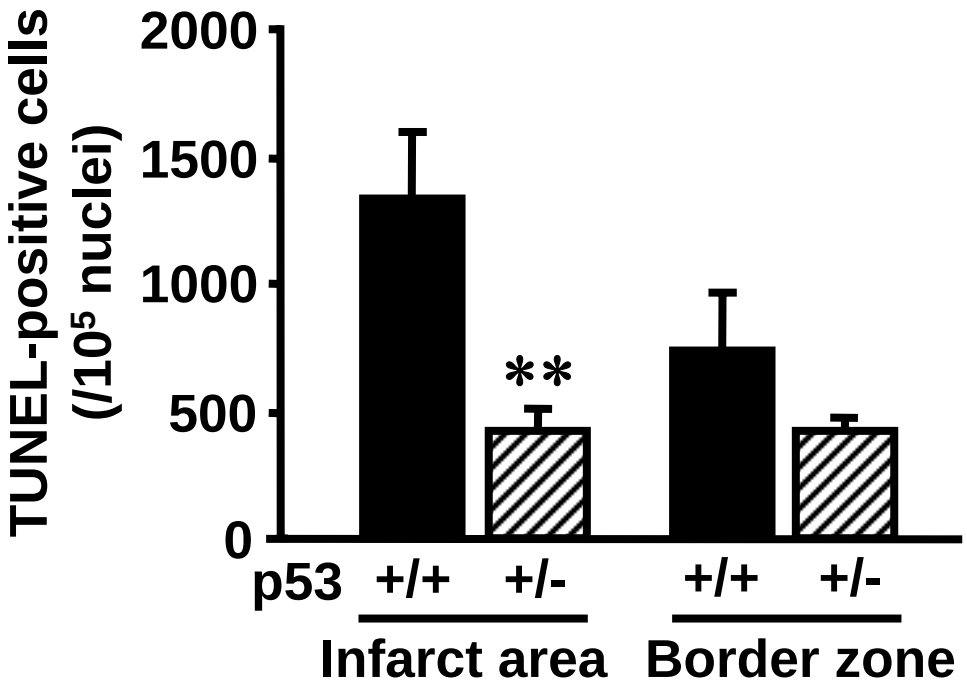
TUNEL-positive cells
(/10^5 nuclei)
2000
1500
1000
500
0
**
p53 +/+ +/- +/+ +/-
Infarct area
Border zone

B

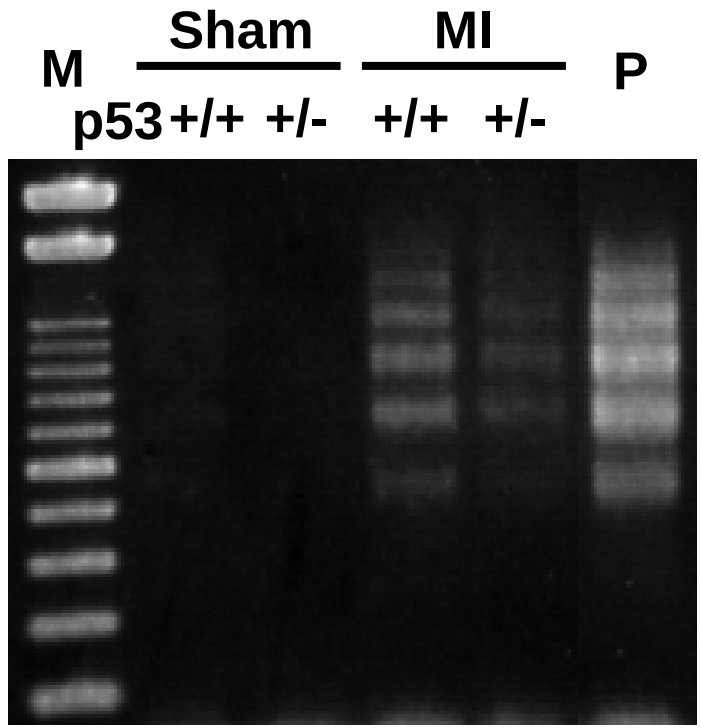
M
Sham
MI
P
p53 +/+ +/- +/+ +/-

Table 1. Echocardiographic and Hemodynamic Data at 3 Days After Surgery

	$p53^{+/+}$+Sham	**$p53^{+/-}$+Sham**	**$p53^{+/+}$+MI**	**$p53^{+/-}$+MI**
Echocardiographic data				
n	7	7	13	12
Heart rate, bpm	491±3	487±5	492±7	493±5
LVEDD, mm	3.7±0.1	3.7±0.1	4.6±0.1**	4.7±0.1**
LVESD, mm	2.3±0.0	2.3±0.1	3.9±0.1**	3.8±0.1**
Fractional shortening, %	36.6±0.4	37.7±0.4	16.5±1.0**	17.9±0.7**
Hemodynamic data				
n	7	7	11	10
Heart rate, bpm	492±14	491±10	481±15	490±13
Mean aortic pressure, mmHg	79±4	79±2	77±2	79±2
LVEDP, mmHg	1.3±0.4	1.3±0.4	12.0±1.9**	11.7±2.9**
$LVdP/dt_{max}$, mmHg/sec	9055±1133	8299±332	5927±409**	5710±240**

MI, myocardial infarction. LV, left ventricular. EDD, end-diastolic diameter. ESD, end-systolic diameter. EDP, end-diastolic pressure. bpm, beats per min.

Values are means±SEM. ** $P<0.01$ vs. $p53^{+/+}$+Sham.